Microglial activation correlates with severity in Huntington disease

A clinical and PET study

N. Pavese, MD; A. Gerhard, MD*; Y.F. Tai, MRCP*; A.K. Ho, PhD; F. Turkheimer, PhD; R.A. Barker, PhD; D.J. Brooks, MD, DSc; and P. Piccini, MD, PhD

Abstract—*Background:* Huntington disease (HD) is characterized by the progressive death of medium spiny dopamine receptor bearing striatal GABAergic neurons. In addition, microglial activation in the areas of neuronal loss has recently been described in postmortem studies. Activated microglia are known to release neurotoxic cytokines, and these may contribute to the pathologic process. *Methods:* To evaluate in vivo the involvement of microglia activation in HD, the authors studied patients at different stages of the disease using [^{11}C](*R*)-PK11195 PET, a marker of microglia activation, and [^{11}C]raclopride PET, a marker of dopamine D2 receptor binding and hence striatal GABAergic cell function. *Results:* In HD patients, a significant increase in striatal [^{11}C](*R*)-PK11195 binding was observed, which significantly correlated with disease severity as reflected by the striatal reduction in [^{11}C]raclopride binding, the Unified Huntington's Disease Rating Scale score, and the patients' CAG index. Also detected were significant increases in microglia activation in cortical regions including prefrontal cortex and anterior cingulate. *Conclusions:* These [^{11}C](*R*)-PK11195 PET findings show that the level of microglial activation correlates with Huntington disease (HD) severity. They lend support to the view that microglia contribute to the ongoing neuronal degeneration in HD and indicate that [^{11}C](*R*)-PK11195 PET provides a valuable marker when monitoring the efficacy of putative neuroprotecting agents in this relentlessly progressive genetic disorder.

NEUROLOGY 2006;66:1638–1643

The mechanisms underlying neuronal death in Huntington disease (HD) are still unknown. Two recent articles have reported the presence of activated microglia in postmortem HD brain.[1,2] It is unclear whether glial activation plays a role in cell death, but it has been suggested that whereas microglial activation is unlikely to initiate neuronal death, it could contribute to the neurodegenerative processes by releasing proinflammatory cytokines such as tumor necrosis factor-α, interleukin-1β, interferon-γ, which contribute to the disease progression.[3-5] If microglial activation plays a role in the pathophysiology of HD, this could provide a basis for new therapeutic interventions that block this immune response and alter the progression of the disease.

[^{11}C](*R*)-PK11195 PET is a selective in vivo marker of activated microglia. The peripheral benzodiazepine binding sites for the isoquinoline [^{11}C](*R*)-PK11195 are expressed by the mitochondrial membranes of activated but not resting microglia/brain macrophages.[6] [^{11}C]Raclopride PET ,a marker of the dopamine D2 receptor availability, has been used to measure striatal functional integrity in HD.[7-11] Reductions of [^{11}C]raclopride binding reflect both loss and dysfunction of striatal neurons and correlate with the patients' disability.[7-9,11]

In this study, we sought to 1) determine in vivo the extent of microglial activation in the brain of HD patients and 2) investigate the association between striatal microglial activation, neuronal dysfunction as evidenced by loss of D2 site binding, and clinical ratings of disease severity in HD.

Methods. *Subjects.* Eleven symptomatic HD patients were recruited for the study (table 1). All these patients had genetically proven disease with an expanded CAG repeat in the *IT15* gene on chromosome 4. All patients had been tested previously at an earlier stage of their disease, and no genetic testing was repeated for this study. Three patients had their genetic test reported as ">36," whereas the effective length of the CAG repeat was available for the remaining patients allowing us to calculate their CAG index,[12] a measure of striatal dysfunction, according to the following formula: striatal dysfunction = constant × age × (CAG – 35.5).

Patients' motor disability was rated with the Unified Huntington's Disease Rating Scale (UHDRS) Total Motor score [13] (ranging from 0 = no signs of HD to 124 = worst score) by an independent scorer who was blinded to the PET data.

Ten healthy volunteers (5 men, 5 women; mean ± SD age

*These authors contributed equally to this article.

From the MRC Clinical Sciences Centre and Division of Neuroscience (N.P., A.G., Y.F.T., F.T., D.J.B., P.P.), Faculty of Medicine, Imperial College, Hammersmith Hospital, London, and Centre for Brain Repair and Department of Neurology (A.K.H., R.A.B.), University of Cambridge, UK.

A. Gerhard was funded by the PDS UK (MAP 02/04). Y.F. Tai is funded by the Wellcome Trust. A.K. Ho was funded by the Medical Research Council.

Disclosure: The authors report no conflicts of interest.

Received June 30, 2005. Accepted in final form February 17, 2006.

Address correspondence and reprint requests to Dr. P. Piccini, Hammersmith Hospital, DuCane Road, Cyclotron Bldg., W12 0NN, London, UK; e-mail: paola.piccini@csc.mrc.ac.uk

Table 1 *Clinical characteristics of the 11 patients with Huntington disease*

Case no.	Sex	Age, y	CAG repeat	Disease duration, y*	UHDRS Motor score,†	Treatment
1	M	44	>36	6	4	No
2	M	47	45	9	4	No
3	F	43	51	NA	28	No
4	F	39	>36	6	30	No
5	M	47	47	6	12	Neuroleptics
6	F	52	>36	9	16	No
7	M	44	41	7	3	No
8	M	45	40	1	0	No
9	F	49	42	10	14	No
10	M	49	44	8	31	No
11	M	68	45	8	35	Neuroleptics
		47.9 ± 7.5		5.2 ± 4.1		

* Based on patient's recollection of first symptoms.
† Best possible score = 0, worst possible score = 124.

NA = the patient was not able to recall the onset of her symptoms; UHDRS = Unified Huntingdon's Disease Rating Scale.

57.4 ± 11.3 years) were used as controls for the [^{11}C](*R*)-PK11195 PET studies and 10 healthy volunteers (8 men, 2 women; mean ± SD age 46.7 ± 14.1 years) were controls for the [^{11}C]raclopride PET studies.

PET methodology. This study received approval from the Ethics Committee of Hammersmith, Queen Charlotte's and Chelsea and Acton Hospitals Trust. Permission to administer [^{11}C](*R*)-PK11195 and [^{11}C]raclopride was obtained from the Administration of Radioactive Substances Advisory Committee of the United Kingdom.

Nine patients were studied with both [^{11}C](*R*)-PK11195 and [^{11}C]raclopride PET 1 week apart, whereas two patients only had an [^{11}C](*R*)-PK11195 study as they were receiving D2 blocking neuroleptics. None of the nine patients who had both scans was taking medication known to affect clinical status or to alter the binding of the radioactive tracers used for PET scanning (benzodiazepine, tetrabenazine, neuroleptics, or *N*-methyl-D-aspartate receptor blocking agents) at any time during the study. In addition, none of the patients in the study was taking anti-inflammatory medications.

Normal healthy volunteers and HD patients were scanned using an ECAT EXACT HR++ (CTI/Siemens 966; Siemens, Knoxville, TN) PET tomograph with a total axial field of view of 23.4 cm. The tomograph has a transaxial spatial resolution of 4.8 ± 0.2 mm and axial resolution of 5.6 ± 0.5 mm after image reconstruction.[14] For [^{11}C](*R*)-PK11195, a mean dose of 294 MBq (range 292 to 300 MBq) was administered IV over 30 seconds. Dynamic data were collected over 60 minutes as 18 time frames. The mean tracer dose for [^{11}C]raclopride was 183 MBq (range 180 to 186 MBq). Scanning began at the start of tracer infusion, generating 20 time frames over 65 minutes.

PET analysis. Parametric images of [^{11}C](*R*)-PK11195 binding potential (BP), reflecting B_{max}/K_d, were generated with the simplified tissue reference compartmental model. As HD has a widespread distribution of pathologic changes, finding a reference region free of disease can be difficult. Cluster analysis was therefore used to extract and identify a distributed cluster of voxels that mirrored a normal population cortical reference input function for individual HD cases, as previously described.[6,15,16] In brief, voxels in the raw dynamic data were segmented into 10 clusters distinguished by the shape of their time–activity curves (TACs).[6] In normal brain, 90% of the voxels segregate into two clusters: one representing a TAC with the shape of the ligand kinetic as seen in normal healthy cortex and the other representing a TAC mainly from extracerebral structures. The patient cluster representing a "normal" cortical reference TAC was tested for dissimilarity with a previously established normal mean population input TAC (χ^2 test, $p < 0.05$). HD patient reference clusters contained mainly cortical voxels.

Parametric images of [^{11}C]raclopride BP were generated from the dynamic scan series using a basis function implementation of the simplified reference region compartmental model with the cerebellum providing the reference tissue input function.[17]

Parametric images of [^{11}C]raclopride and [^{11}C](*R*)-PK11195 BP for each subject were anatomically coregistered and resliced to their respective T1-weighted MRI using the Mutual Information Registration algorithm in the SPM'99 software package (Wellcome Department of Cognitive Neuroscience, Institute of Neurology, London, UK) implemented in Matlab5.

BP values for the whole striatum, caudate, putamen, and pallidum were obtained by defining regions of interest (ROIs) on the individual MR images that were subsequently used to sample the parametric images. For each patient, the left to right averaged striatum, putamen, and caudate BPs were calculated.

Extrastriatal regions. Two methods of analysis were employed to evaluate the extent of microglial activation in the extrastriatal regions: 1) the ROI approach and 2) statistical parametric mapping (SPM), which allows exploratory group comparisons at a voxel level throughout the entire brain volume without requiring an a priori hypothesis.

To extract extrastriatal ROI data, we applied a standard object map to spatially transformed parametric images of [^{11}C](*R*)-PK11195 BP. The standard object map contained regions defined for hypothalamus, frontal, parietal, temporal, and occipital lobes that had been traced free hand onto the Montreal Neurologic Institute (MNI) single-subject MRI in standard space found in the SPM'99 package using ANALYZE software (Analyze AVW, Mayo Clinic).

Stereotaxic image transformation involved spatial normalization of individual parametric images of [^{11}C](*R*)-PK11195 BP into standard MNI space. This was done by first normalizing the individual's T1-weighted MRI to the template in MNI space available in SPM'99 and then applying the transformation parameters to the respective BP images previously coregistered to individual's T1-weighted MRI. In one patient, the spatial normalization of her MRI to the MNI template was unsuccessful, and this patient was excluded from the analysis.

SPM was performed using the SPM'99 software package. Normalized [^{11}C](*R*)-PK11195 parametric images were spatially smoothed using a 6 × 6 × 6 mm (full-width at half maximum) isotropic Gaussian kernel.

Between-group comparisons of [^{11}C](*R*)-PK11195 binding in HD patients and normal subjects were performed by using a weighted contrast to localize significant increases in mean voxel BP values in HD. The contrast was used to generate maps of *Z* scores on a voxel basis using the general linear model.[18] The statistical maps were visualized at a threshold of $p < 0.01$ (*Z* score = 2.33), and any resulting clusters with a $p < 0.05$ are reported.

Table 2 *Mean [^{11}C](R)-PK11195 binding potential in striatal and extrastriatal areas in Huntington disease patients compared with healthy volunteers*

	Healthy volunteers, n = 10	Huntington disease patients, n = 10
Caudate	0.08 ± 0.01	0.20 ± 0.03†
Putamen	0.18 ± 0.01	0.34 ± 0.04†
Pallidum	0.22 ± 0.02	0.44 ± 0.04†
Hypothalamus	0.42 ± 0.08	0.36 ± 0.08
Frontal lobe	0.15 ± 0.01	0.19 ± 0.01*
Parietal lobe	0.13 ± 0.01	0.17 ± 0.01*
Temporal lobe	0.15 ± 0.01	0.17 ± 0.01
Occipital lobe	0.17 ± 0.01	0.19 ± 0.01

Values are means ± SE.

* $p < 0.05$; † $p < 0.01$.

Statistical analysis. Statistical analyses of clinical data were performed with InStat3 for Macintosh (University of Medicine and Dentistry, Piscataway, NJ). Comparisons between groups were made using a nonparametric unpaired test (Mann–Whitney statistic). Linear regressions were used for correlations between BP values and variables of interest.

Results. *[^{11}C](R)-PK11195 PET findings.* The HD patients, compared with a group of normal subjects, showed increased mean [^{11}C](*R*)-PK11195 BP levels in the whole striatum (0.31 ± 0.03 vs ± 0.013 ± 0.013 mean ± SE; $p < 0.001$), caudate (0.20 ± 0.03 vs 0.08 ± 0.01; $p < 0.01$), putamen (0.34 ± 0.04 vs 0.18 ± 0.01; $p < 0.01$), and pallidum (0.44 ± 0.04 vs 0.22 ± 0.02; $p < 0.01$).

Significant increases in mean [^{11}C](*R*)-PK11195 BP were also observed in frontal and parietal ROIs of HD patients compared with the normal subjects.

The results of the ROI analysis are summarized in table 2.

SPM categorical comparisons between control and HD groups localized clusters of significant bilateral increases in mean [^{11}C](*R*)-PK11195 BP in striatum, pallidum, thalamus, frontal areas, and the insulae (table 3; figure 1) of the HD cohort.

[^{11}C]Raclopride PET findings. Mean whole striatum, caudate, and putamen [^{11}C]raclopride BP values were decreased ($p < 0.001$) in the HD patients compared with the normal subjects (striatum 1.49 ± 0.12 vs 3.51 ± 0.4; caudate 1.38 ± 0.14 vs 3.21 ± 0.29 and putamen 1.54 ± 0.11 vs 3.62 ± 0.3). The normal mean striatal [^{11}C]raclopride BP values were similar to those reported in previous studies from this unit.[19-21]

Figure 2 shows [^{11}C](*R*)-PK11195 and [^{11}C]raclopride PET BP maps from a HD patient (Patient 3) and a normal subject.

Figure 3 shows scatter plots of individual HD and control BPs for each of the two ligands.

Clinical correlations. Within the HD cohort, higher individual striatal [^{11}C](*R*)-PK11195 BPs correlated with lower striatal [^{11}C]raclopride BPs ($r = -0.69$, $p < 0.05$) (figure 4A). In the subgroup of patients where the exact CAG repeat length was available, higher individual striatal [^{11}C](*R*)-PK11195 BPs also correlated with higher CAG indexes ($r = 0.90$, $p < 0.01$) (figure 4B).

Clinical severity, assessed with the UHDRS, correlated with both striatal [^{11}C]raclopride BP ($r = -0.77$, $p < 0.05$) and striatal [^{11}C](*R*)-PK11195 BP values ($r = 0.69$, $p <$

Table 3 *Areas of significant increases in [^{11}C](R)-PK11195 binding potential in Huntington disease patients compared with healthy volunteers*

Z score	Talairach coordinates *x*	*y*	*z*	Area	*p* Value corrected
3.67	20	4	−2	R putamen	<0.001
3.58	−16	−19	1	L thalamus	<0.001
3.57	14	14	3	R caudate	<0.001
3.38	−23	−2	−1	L putamen	<0.001
3.38	−16	−4	−2	L pallidum	<0.001
3.24	−14	10	10	L caudate	<0.001
3.22	12	2	−5	R pallidum	<0.001
3.11	18	−13	6	R thalamus	<0.001
3.11	51	1	18	R inferior frontal gyrus	<0.001
3.10	16	54	−3	R medial frontal gyrus	<0.001
3.08	−44	20	10	L inferior frontal gyrus	<0.001
3.05	57	2	7	R precentral gyrus	<0.001
3.0	−14	47	0	L anterior cingulate	<0.001
2.64	18	45	−2	R anterior cingulate	<0.01
2.59	−36	14	10	L insula	<0.01
2.52	−42	10	7	L precentral gyrus	<0.01

Coordinates are from the brain atlas of Talairach and Tournoux.[35]

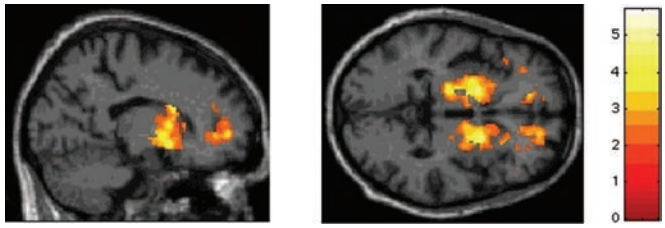

Figure 1. Increased microglia activation in Huntington disease patients. Sagittal (x = 17) and transaxial (z = −2) projections of statistical parametric maps showing areas of significant increases in [^{11}C](R)-PK11195 binding potential in the patients with Huntington disease (n = 10) compared with normal subjects (n = 10). In the sagittal image, increases are seen in the right caudate (x = 18, y = 14, z = 3), right putamen (x = 18, y = 4, z = –2), and right anterior cingulate (x = 18, y = 45, z = –2). In the transaxial image, increases are seen in the right (x = 14, y = 14, z = −2) and left (x = −14, y = −10, z = –2) caudate, right (x = 20, y = 4, z = −2) and left (x = −23, y = −2, z = –2) putamen, right (x = 12, y = 2, z = –2) and left (x = −16, y = −4, z = –2) pallidum, and right (x = 18, y = 45, z = –2) and left (x = −14, y = 47, z = –2) anterior cingulate. The color stripe indicates t values. Areas are superimposed on the normalized T1-weighted MRI of one of the Huntington disease patients.

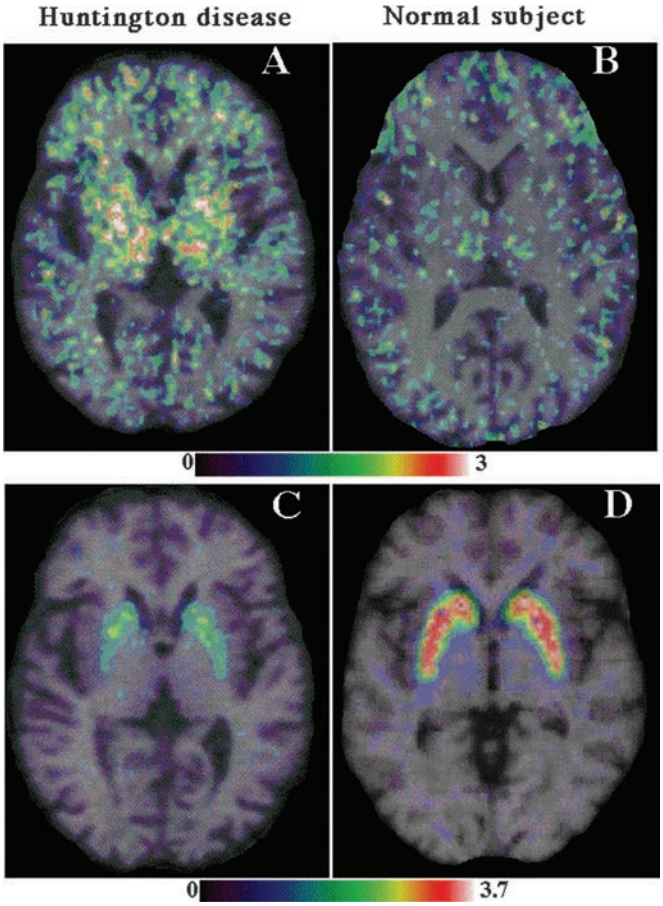

Figure 2. [^{11}C](R)-PK11195 (A and B) and [^{11}C]raclopride (C and D) PET binding potential maps from a Huntington disease patient (Patient 3) (left) and a normal subject (right). The color stripes indicate binding potential values for [^{11}C](R)-PK11195 (top) and [^{11}C]raclopride (bottom).

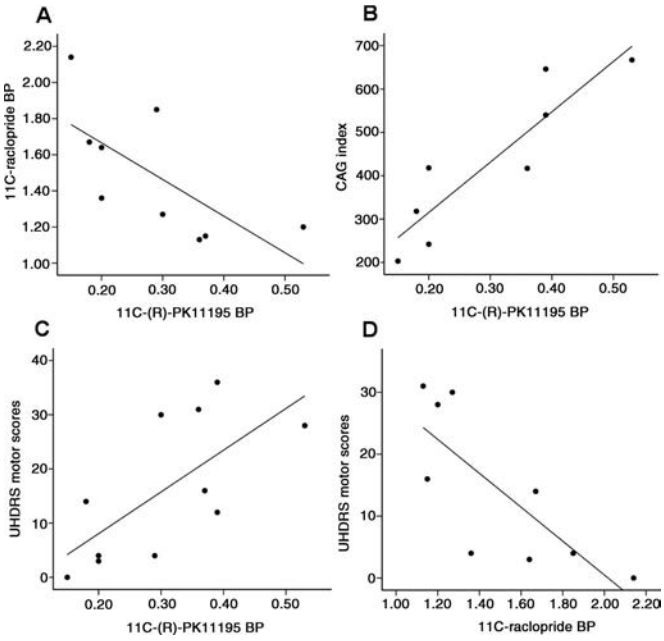

Figure 4. Activated microglia and measurements of disease severity in Huntington disease patients. (A) Correlation between striatal values of [^{11}C](R)-PK11195 and [^{11}C]raclopride binding potential (correlation coefficient $r = -0.68$, $p < 0.05$). (B) Correlation between striatal values of [^{11}C](R)-PK11195 and CAG indexes (correlation coefficient $r = 0.90$, $p < 0.01$). (C) Correlation between striatal values of [^{11}C](R)-PK11195 and Unified Huntingdon's Disease Rating Scale (UHDRS) scores (correlation coefficient $r = 0.69$, $p < 0.05$). (D) Correlation between striatal values of [^{11}C]raclopride and UHDRS scores (correlation coefficient $r = -0.77$, $p < 0.05$).

0.05), indicating that worse individual UHDRS scores correlated with lower striatal [^{11}C]raclopride BPs and with higher individual striatal [^{11}C](*R*)-PK11195 BPs (figure 4, C and D).

Discussion. In this in vivo PET study, we found significant increases in [^{11}C](*R*)-PK11195 binding in the striatum and in extrastriatal areas (frontal and parietal cortex) of HD patients compared with normal control subjects. Observer independent SPM confirmed and extended the ROI analysis by localizing clusters of significant bilateral increases in [^{11}C](*R*)-PK11195 BP in neostriatum, pallidum, frontal cortex, anterior cingulated, and insulae in these same HD patients. Interestingly, there was no significant difference between the two groups in [^{11}C](*R*)-PK11195 binding in the hypothalamus, a structure reported to be severely affected in HD.[22] It should be noticed, however, that the BP values in the hypothalamus are probably overestimated owing to the spillover from the thalamus, which usually has high levels of activated microglia even in normal subjects.

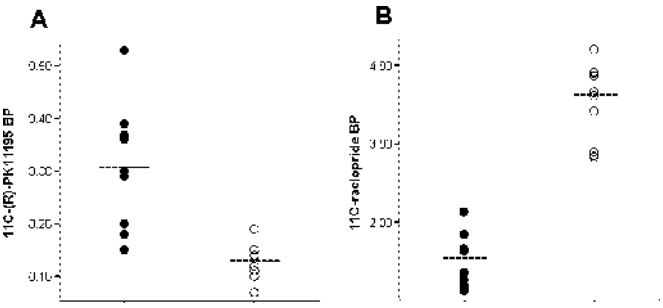

Figure 3. Scatterplots of Huntington disease patients and normal subjects' binding potential values of [^{11}C](R)-PK11195 (A) and [^{11}C]raclopride (B). Filled circles represent individual Huntington disease patients and open circles represent normal subjects.

Our in vivo PET results are in line with the findings of two postmortem studies in HD[1,2] where activated microglia were observed in neostriatum,[1,2] globus pallidus,[2] and in Brodmann areas 9 and 10 of the frontal cortex but show more extensive disease activity.

In one study,[2] the density of reactive microglia was related to the degree of neuronal loss, but no premortem clinical data were available. In our HD cohort, we have demonstrated that higher individual BP values of [^{11}C](*R*)-PK11195 correlated with lower BP values of [^{11}C]raclopride in striatum and with higher CAG indexes, another measurement of striatal dysfunction.[12] Finally, we have shown that higher

UHDRS scores correlated with higher striatal BP values of [^{11}C](R)-PK11195. Taken together, these results suggest a close association between level of microglial activation and severity of clinical disease.

We found that the location of increased cortical [^{11}C](R)-PK11195 binding in our HD patients corresponds well with the known distribution of neuronal loss in the disease.[23] Activated microglia were particularly evident in the frontal cortex of these patients. Interestingly, symptoms of frontal lobe involvement occur early in HD and sometimes can precede the motor symptoms of the disease, although reductions of frontal lobe volume, metabolism, and blood flow have not consistently been found in HD patients with mild to moderate clinical disease.[24-29] Given this, [^{11}C](R)-PK11195 PET may represent a more sensitive in vivo marker of "ongoing" pathology in cortical areas in HD with respect to these other imaging techniques.

Activation of microglia in response to acute and chronic brain insults is in part an attempt of the body to initiate reparative measures in the affected areas. These cells, in fact, are able to support neuronal survival by releasing growth factors and contributing to remodeling of synapses.[30,31] However, there is cumulative evidence suggesting that activated microglia also result in neuronal death through the release of a variety of immune cytokines and other neurotoxic factors.[3-5] It is likely that in conditions characterized by extensive chronic microglial activation, these harmful effects overwhelm the beneficial ones, leading to a self-propagating cycle where activated microglia promote further neurodegeneration and subsequent further induction of microglia activation and production of neurotoxic factors. Our finding of significantly increased levels of microglia activation in HD striatum, which correlated with measures of disease severity, supports this view. Our findings also suggest that activation of microglia occurs in the early stages of HD. Two of our patients showed increased binding of striatal [^{11}C](R)-PK11195 and reduced dopamine D2 receptor function despite very mild clinical involvement (Patients 1 and 8). It has been previously reported that reduced striatal dopamine receptor function can be seen in the presymptomatic phase of the disease.[10]

The exact role of activated microglia in the neurodegenerative process of HD, however, remains to be clarified, as we cannot exclude the possibility that it is just a "bystander effect" of neuronal death. Further studies in preclinical HD gene carriers will increase our knowledge concerning the extent of microglial activation in the early stages of the disease and the temporal relationship between microglial activation and HD pathology.

Finally, it may be argued that the atrophy reported in active HD could confound quantification of the functional PET data in our study. However, as we have found increased [^{11}C](R)-PK11195 binding in the HD patients compared with controls despite any partial volume effects due to atrophy, the corrected [^{11}C](R)-PK11195 BPs would be, if anything, even higher. Conversely, partial volume effects due to brain atrophy could result in our underestimating striatal [^{11}C]raclopride BPs in our patients. As we are using [^{11}C]raclopride as an in vivo marker of striatal degeneration, the extent to which reductions in measured BP are due to volume effects as opposed to loss of function within remaining neuron is semantic as both these processes reflect underlying disease progression.

Taken together, our results show that [^{11}C](R)-PK11195 PET, although not disease specific, provides a valid in vivo marker of the microglial activation occurring in HD. The close association between microglia activation, neuronal dysfunction, and clinical disability in our patients lends support to the view that activated microglia contribute to the pathology of HD. It also suggests that microglial activation is likely to increase over the time course of the disease. Longitudinal clinical studies will further elucidate the temporal relationship between these two processes and will give more information on whether the progressive increase in microglia activation occurs in a linear or nonlinear fashion.

In the future, longitudinal assessment with [^{11}C](R)-PK11195 PET in clinical trials could be of value in demonstrating the mechanistic effects of putative neuroprotective agents such as minocycline[32-34] and anti-inflammatory agents in HD.

Acknowledgment

The authors thank Hope McDevitt, Stella Ahier, Andreana Williams, and Andrew Blyth for help with scanning and L. Schnorr for technical assistance with PET data reconstruction. N.P. acknowledges Prof. R.Y. Moore, Dr. Gary Hotton, Dr. Nobukatsu Sawamoto, and Dr. Philippe Remy for criticism and suggestions in data analysis.

References

1. Messmer K, Reynolds GP. Increased peripheral benzodiazepine binding sites in the brain of patients with Huntington's disease. Neurosci Lett 1998;241:53–56.
2. Sapp E, Kegel KB, Aronin N, et al. Early and progressive accumulation of reactive microglia in the Huntington disease brain. J Neuropathol Exp Neurol 2001;60:161–172.
3. Wilms H, Sievers J, Dengler R, et al. Intrathecal synthesis of monocyte chemoattractant protein-1 (MCP-1) in amyotrophic lateral sclerosis: further evidence for microglial activation in neurodegeneration. J Neuroimmunol 2003;144:139–142.
4. Melton LM, Keith AB, Davis S, et al. Chronic glial activation, neurodegeneration, and APP immunoreactive deposits following acute administration of double-stranded RNA. Glia 2003;44:1–12.
5. Nakanishi H. Microglial functions and proteases. Mol Neurobiol 2003; 27:163–176.
6. Banati RB, Newcombe J, Gunn RN, et al. The peripheral benzodiazepine binding site in the brain in multiple sclerosis: quantitative in vivo imaging of microglia as a measure of disease activity. Brain 2000;123: 2321–2337.
7. Turjanski N, Weeks R, Dolan R, et al. Striatal D_1 and D_2 receptor binding in patients with Huntington's disease and other choreas: a PET study. Brain 1995;118:689–696.
8. Ginovart N, Lundin A, Farde L, et al. PET study of the pre- and post-synaptic dopaminergic markers for the neurodegenerative process in Huntington's disease. Brain 1997;120:503–514.
9. Antonini A, Leenders KL, Eidelberg D. [11C] Raclopride-PET studies of the Huntington's disease rate of progression: relevance of the trinucleotide repeat length. Ann Neurol 1998;43:253–255.
10. Andrews TC, Weeks RA, Turjanski N, et al. Huntington's disease progression PET and clinical observations. Brain 1999;122:2353–2363.

11. Pavese N, Andrews TC, Brooks DJ, et al. Progressive striatal and cortical dopamine receptor dysfunction in Huntington's disease: a PET study. Brain 2003;126:1127–1135.
12. Penney JB Jr, Vonsattel JP, MacDonald ME, Gusella JF, Myers RH. CAG repeat number governs the development rate of pathology in Huntington's disease. Ann Neurol 1997;41:689–692.
13. Huntington Study Group. Unified Huntington's Disease Rating Scale: reliability and consistency. Mov Disord 1996;11:136–142.
14. Spinks TJ, Jones T, Bloomfield PM, et al. Physical characteristics of the ECAT EXACT 3D positron tomograph. Phys Med Biol 2000;45:2601–2618.
15. Cagnin A, Myers R, Gunn RN, et al. In vivo visualization of activated glia by [11C] (R)-PK11195-PET following herpes encephalitis reveals projected neuronal damage beyond the primary focal lesion. Brain 2001; 124:2014–2027.
16. Gerhard A, Banati RB, Goerres GB, et al. [11C](R)-PK11195 PET imaging of microglial activation in multiple system atrophy. Neurology 2003; 61:686–689.
17. Gunn RN, Lammertsma AA, Hume SP, Cunningham VJ. Parametric imaging of ligand–receptor binding in PET using a simplified reference region model. Neuroimage 1997;6:279–287.
18. Friston KJ, Holmes AP, Worsley KJ, et al. Statistical parametric maps in functional imaging: a general linear approach. Hum Brain Map 1995; 2:189–210.
19. Piccini P, Brooks DJ, Bjorklund A, et al. Dopamine release from nigral transplants visualized in vivo in a Parkinson's patient. Nat Neurosci 1999;2:1137–1140.
20. Goerendt IK, Messa C, Lawrence AD, et al. Dopamine release during sequential finger movements in health and Parkinson's disease: a PET study. Brain 2003;126:312–325.
21. Scherfler C, Khan NL, Pavese N, et al. Striatal and cortical pre- and post-synaptic dopaminergic dysfunction in sporadic *parkin*-linked parkinsonism. Brain 2004;127:1332–1342.
22. Petersen A, Gil J, Maat-Schieman ML, et al. Orexin loss in Huntington's disease. Hum Mol Genet 2005;14:39–47.
23. Heinsen H, Strik M, Bauer M, et al. Cortical and striatal neurone number in Huntington's disease. Acta Neuropathol (Berl) 1994;88:320–333.
24. Kuhl DE, Phelps ME, Markham CH, Metter EJ, Riege WH, Winter J. Cerebral metabolism and atrophy in Huntington's disease determined by 18FDG and computed tomographic scan. Ann Neurol 1982;12:425–434.
25. Tanahashi N, Meyer JS, Ishikawa Y, et al. Cerebral blood flow and cognitive testing correlate in Huntington's disease. Arch Neurol 1985; 42:1169–1175.
26. Young AB, Penney JB, Starosta-Rubinstein S, et al. PET scan investigations of Huntington's disease: cerebral metabolic correlates of neurological features and functional decline. Ann Neurol 1986;20:296–303.
27. Weinberger DR, Berman KF, Iadarola M, Driesen N, Zec RF. Prefrontal cortical blood flow and cognitive function in Huntington's disease. J Neurol Neurosurg Psychiatry 1988;51:94–104.
28. Sax DS, Powsner R, Kim A, et al. Evidence of cortical metabolic dysfunction in early Huntington's disease by single-photon-emission computed tomography. Mov Disord 1996;11:671–677.
29. Aylward EH, Codori AM, Barta PE, Pearlstein GD, Harris GJ, Brandt J. Basal ganglia volume and proximity to onset in presymptomatic Huntington's disease. Arch Neurol 1996;53:1293–1296.
30. Streit WJ. Microglia as neuroprotective, immunocompetent cells of the CNS. Glia 2002;40:133–139.
31. Kim SU, de Vellis J. Microglia in health and disease. J Neurosci Res 2005;81:302–313.
32. Bonelli RM, Heuberger C, Reisecker F. Minocycline for Huntington's disease: an open label study. Neurology 2003;60:883–884.
33. Huntington Study Group. Minocycline safety and tolerability in Huntington disease. Neurology 2004;63:547–549.
34. Thomas M, Ashizawa T, Jankovic J. Minocycline in Huntington's disease: a pilot study. Mov Disord 2004;19:692–695.
35. Talairach J, Tournoux P.A coplanar sterotactic atlas of the human brain. New York: Thieme, 1988.